

## Reassessment of the transport mechanism of the human zinc transporter SLC39A2

Marie Christine Franz, Jonai Pujol-Gimenez, Nicolas Montalbetti, Miguel Fernandez-Tenorio, Timothy R. DeGrado, Ernst Niggli, Michael F. Romero, and Matthias A. Hediger

*Biochemistry*, **Just Accepted Manuscript** • DOI: 10.1021/acs.biochem.8b00511 • Publication Date (Web): 23 May 2018

Downloaded from <http://pubs.acs.org> on May 25, 2018

### Just Accepted

“Just Accepted” manuscripts have been peer-reviewed and accepted for publication. They are posted online prior to technical editing, formatting for publication and author proofing. The American Chemical Society provides “Just Accepted” as a service to the research community to expedite the dissemination of scientific material as soon as possible after acceptance. “Just Accepted” manuscripts appear in full in PDF format accompanied by an HTML abstract. “Just Accepted” manuscripts have been fully peer reviewed, but should not be considered the official version of record. They are citable by the Digital Object Identifier (DOI®). “Just Accepted” is an optional service offered to authors. Therefore, the “Just Accepted” Web site may not include all articles that will be published in the journal. After a manuscript is technically edited and formatted, it will be removed from the “Just Accepted” Web site and published as an ASAP article. Note that technical editing may introduce minor changes to the manuscript text and/or graphics which could affect content, and all legal disclaimers and ethical guidelines that apply to the journal pertain. ACS cannot be held responsible for errors or consequences arising from the use of information contained in these “Just Accepted” manuscripts.



1  
2  
3  
4  
5 **Reassessment of the transport mechanism of the human zinc transporter**  
6 **SLC39A2**  
7

8  
9 **Marie C. Franz<sup>1,4,#</sup>, Jonai Pujol-Giménez<sup>1,#</sup>, Nicolas Montalbetti<sup>1,5)</sup>, Miguel Fernandez-**  
10 **Tenorio<sup>2)</sup>, Timothy R. DeGrado<sup>3)</sup>, Ernst Niggli<sup>2)</sup>, Michael F. Romero<sup>3)</sup> and Matthias A. Hediger<sup>1,\*</sup>**  
11  
12  
13  
14

15 **# Both authors contributed equally to this work**  
16

17 **\* Corresponding Author:**

18 Matthias A. Hediger

19 Institute of Biochemistry and Molecular Medicine

20 University of Bern, Bülhstrasse 28

21 3012 Bern

22 Switzerland

23 Tel: +41 31 631 41 29

24 Email: [Matthias.hediger@ibmm.unibe.ch](mailto:Matthias.hediger@ibmm.unibe.ch)  
25  
26  
27  
28  
29  
30

31 <sup>1)</sup> University of Bern, Institute of Biochemistry and Molecular Medicine and National Center of  
32 Competence in Research, NCCR TransCure, Bülhstrasse 28, 3012 Bern, Switzerland.

33 <sup>2)</sup> University of Bern, Department of Physiology, Buehlplatz 5, 3012 Bern, Switzerland

34 <sup>3)</sup> Mayo Clinic College of Medicine and Science, Department of Physiology and Biomedical Engineering,  
35 Mayo Clinic Joseph Building, Rochester, MN 55905, USA

36 <sup>4)</sup> Current address: CSL Behring, Wankdorfstrasse 10, 3014 Bern, Switzerland

37 <sup>5)</sup> Current address: University of Pittsburgh, Department of Medicine, 3550 Terrace Street, Pittsburgh, PA  
38 15261, USA.  
39  
40  
41  
42  
43  
44  
45  
46  
47  
48  
49  
50  
51  
52  
53  
54  
55  
56  
57  
58  
59  
60

## Abstract

The human zinc transporter SLC39A2, also known as ZIP2, was shown to mediate zinc transport that could be inhibited at pH values below 7.0 and stimulated by  $\text{HCO}_3^-$ , suggesting a  $\text{Zn}^{2+}/\text{HCO}_3^-$  cotransport mechanism (1). In contrast, recent experiments in our laboratory indicated that the functional activity of ZIP2 increases at acidic pH (2). The present study was therefore designed to reexamine the findings on the pH-dependence and to extend the functional characterization of ZIP2.

Our current results show that ZIP2-mediated transport is modulated by extracellular pH, but independent of the  $\text{H}^+$  driving force. Also, in our experiments, ZIP2-mediated transport is not modulated by extracellular  $\text{HCO}_3^-$ . Moreover, high extracellular  $[\text{K}^+]$ , which induces depolarization, inhibited ZIP2-mediated transport, indicating that the transport mechanism is voltage-dependent.

We also show that ZIP2-mediates the uptake of  $\text{Cd}^{2+}$  ( $K_m \sim 1.57 \mu\text{M}$ ) in a pH-dependent manner ( $K_{H^+}$  of  $\sim 66 \text{ nM}$ ).  $\text{Cd}^{2+}$  transport is inhibited by extracellular  $[\text{Zn}^{2+}]$  ( $\text{IC}_{50} \sim 0.32 \mu\text{M}$ ),  $[\text{Cu}^{2+}]$  ( $\text{IC}_{50} \sim 1.81 \mu\text{M}$ ) and to a lower extent by  $[\text{Co}^{2+}]$ , but not by  $[\text{Mn}^{2+}]$  or  $[\text{Ba}^{2+}]$ .  $\text{Fe}^{2+}$  is not transported by ZIP2. Accordingly, the substrate selectivity of ZIP2 decreases in the order  $\text{Zn}^{2+} > \text{Cd}^{2+} \geq \text{Cu}^{2+} > \text{Co}^{2+}$ .

Altogether, we propose that ZIP2 is a facilitated divalent metal ion transporter that can be modulated by extracellular pH and membrane potential. Given that ZIP2 expression has been reported in acidic environments (3-5), we suggest that the herein described  $\text{H}^+$ -mediated regulatory mechanism might be important to determine the velocity and direction of the transport process.

## Introduction

Zinc is an essential trace element for human nutrition and the second most abundant transition element after iron in living organisms. The importance of zinc becomes evident when looking at a recent bioinformatics analysis indicating that as much as 10% of the human proteome is potentially capable of binding zinc (6). Over 3000 different types of proteins require zinc as a key structural or catalytic component. Among them are transcription factors, signaling proteins, transport/storage proteins, zinc finger proteins and proteins involved in DNA repair, replication and translation (7). Whole body and cellular zinc homeostasis is being thoroughly regulated. Whereas systemic zinc intoxication is relatively rare, zinc deficiency is a widespread problem leading to growth retardation, cognitive impairment and immune dysfunction (8). Maintenance of mammalian zinc homeostasis is achieved by high-affinity zinc transport systems that are regulated by metal sensors (7). There are at least two different solute carrier (SLC) families of zinc transporters that control  $Zn^{2+}$  movement across membranes: 1) The SLC30 zinc transporter family, also known as ZnT family, that facilitate cellular efflux or uptake into intracellular compartments; and 2) the SLC39 family, also known as ZIP<sup>1</sup> family that facilitates cellular uptake or efflux from intracellular compartments (9-12).

The mammalian SLC39/ZIP family consists of 14 members, which can be divided into four subfamilies based on sequence similarity. SLC39A2 (ZIP2) together with SLC39A1 (ZIP1) and SLC39A3 (ZIP3) comprises subfamily II. ZIP2 was originally cloned and characterized by Gaither and Eide in year 2000 (1). In this study, they showed that ZIP2-expressing K562 cells accumulated more  $^{65}Zn^{2+}$  than parental cells, in a time-, temperature- and concentration-dependent manner. They found that ZIP2-dependent zinc transport was not dependent on ATP hydrolysis and neither on  $Na^+$  or  $K^+$  gradients. In their assay, ZIP2 was inhibited at acidic pH ( $pH < 7.0$ ) and stimulated by 0.5 mM  $HCO_3^-$ . Thus, they proposed a  $Zn^{2+}/HCO_3^-$  cotransport mechanism. In the same study, expression of ZIP2 mRNA was found to be generally low or negligible in human tissues and cultured cell lines, except in prostate and uterus (1), where it indeed could also be detected at the protein level (3). Cao *et al.* found ZIP2 mRNA in peripheral blood mononuclear cells (PBMCs) and monocytes (13). In their study, zinc depletion in both cell lines triggered upregulation of ZIP2 with concomitant downregulation of zinc-binding metallothioneins. Recently, Inoue *et al.* could detect ZIP2 in the epidermis of healthy human frozen skin samples (4). They discovered that ZIP2 was upregulated by differentiation induction of cultured keratinocytes. Interestingly, ZIP2 knockdown inhibited the differentiation of keratinocytes and consequently the formation of a 3D cultured epidermis. Several studies have linked the down-regulation of ZIP2 in prostatic tissue to decreased zinc levels in prostatic epithelial cells and to prostate cancer (3,14-18). Studies with ZIP2-KO

---

<sup>1</sup> ZIP, ZrT/Irt-like protein

1  
2  
3 mice did not reveal any specific phenotype. However, these mice were more susceptible to abnormal  
4 embryonic development due to zinc deficiency during pregnancy (19).  
5

6  
7 Recently, we published a screening assay that was established using the FLIPR Tetra high throughput  
8 microplate reader to identify specific modulators of ZIP2 as potential therapeutic hit or lead compounds  
9 (2). This assay is based on the use of a  $\text{Ca}^{2+}$ -sensitive dye, Calcium 5 (Molecular Devices), which, in  
10 addition to  $\text{Ca}^{2+}$ , binds  $\text{Cd}^{2+}$  with high affinity. Binding of either  $\text{Ca}^{2+}$  or  $\text{Cd}^{2+}$  to the dye induces emission  
11 of a fluorescent signal that can be monitored, allowing quantification of transport activity of proteins that  
12 mediate  $\text{Cd}^{2+}$  influx, such as ZIP2, which transports  $\text{Cd}^{2+}$  efficiently (1,2). In our laboratory, this assay  
13 has been successfully used to monitor the activity of a variety of  $\text{Cd}^{2+}$  transporting proteins such as the  
14 human divalent metal transporter DMT1 (SLC11A2) (20) or the epithelial calcium channel TRPV6 (21).  
15 Interestingly, during the development of the assay, we discovered discrepancies between our results on  
16 ZIP2 transport characteristics and the originally reported functional characterization of ZIP2 (1).  
17 Therefore, the goal of the current work was to reexamine and extend the functional characterization of  
18 ZIP2.  
19  
20  
21  
22  
23  
24  
25

## 26 **Material and Methods**

27  
28 *Chemicals and Reagents* - Unless mentioned, all the chemicals and reagents were purchased from Sigma-  
29 Aldrich  
30

31  
32 *Cell culture methods* - HEK293<sup>2</sup> cells were grown in complete Dulbecco's modified Eagle medium  
33 (Gibco) supplemented with 10% fetal bovine serum (FBS), 10 mM HEPES<sup>3</sup>, 100  $\mu\text{M}$  minimal essential  
34 medium non-essential amino acids and 1 mM sodium pyruvate (Gibco). Cells were cultured at 37 °C and  
35 5 %  $\text{CO}_2$  and subcultivated when confluency reached 90%.  
36  
37

38  
39 Cells were transfected 24h after plating, following the manufacturer's protocol for the Lipofectamine  
40 2000 (Invitrogen) reagent, using 50% of the recommended amount of human SLC39A2/ZIP2 (Uniprot  
41 ID: Q9NP94) encoding DNA and Lipofectamine 2000. The transfection medium was changed after 4 h.  
42 Transfection efficiency was estimated to be at least 70% using fluorescence microscopy.  
43  
44

45  
46  *$\text{Cd}^{2+}$  flux measurements using the FLIPR Tetra* - Cells were plated in 96-well, clear-bottom, black-well  
47 plates coated with poly-D-lysine at a density of  $2 \times 10^4$  cells per well. The next day, cells were transfected  
48 with ZIP2-pIRES2 DsRed-Express2 or mock-transfected using lipotransfection. On the experimental day,  
49 the cell culture medium was replaced with 100  $\mu\text{l}$  of loading buffer (modified Krebs buffer containing 117  
50 mM NaCl, 4,8 mM KCl, 1 mM  $\text{MgCl}_2$ , 10 mM D-Glucose, 5 mM HEPES, 5 mM MES<sup>4</sup> and Calcium-5  
51  
52  
53  
54

55  
56 <sup>2</sup> HEK293, Human embryonic kidney 293

57 <sup>3</sup> HEPES, 4-(2-hydroxyethyl)-1-piperazineethanesulfonic acid

58 <sup>4</sup> MES, 2-(N-Morpholino)ethanesulfonic acid  
59  
60

1  
2  
3  
4 fluorescence dye (Molecular Devices), pH= 6.5). Cells were then incubated in the loading buffer at 37 °C  
5  
6 for 1 h. Fluorescence Cd<sup>2+</sup> measurements were carried out using a FLIPR-Tetra high throughput  
7  
8 fluorescence microplate reader. Cells were excited using the 470–495 nm LED module, and the emitted  
9  
10 fluorescence signal was filtered with a 515–575 nm emission filter. Cd<sup>2+</sup> and the other tested solutes were  
11  
12 prepared in assay buffer as 2x concentrated solutions in a separate 96-well plate. Establishment of a stable  
13  
14 baseline was followed by addition of 100 µl of the indicated [Cd<sup>2+</sup>] and measurements of fluorescence for  
15  
16 15 min. Measurements were made at 1-s intervals. In the negative control group, no substrate was  
17  
18 administered. Results were exported from the FLIPR raw data as “Area Under the Curve” (AUC) of the  
19  
20 fluorescence signal intensity in the interval after the addition of substrates (seconds 460-750). In sodium  
21  
22 replacement experiments 120 mM NaCl were replaced by 120 mM choline chloride, NMDG<sup>5</sup> or KCl. In  
23  
24 chloride replacements assays all the chloride containing salts were replaced by their corresponding  
25  
26 equimolar gluconate salts. In pH-dependence experiments, the different pH were adjusted with 1N  
27  
28 HCl/NaOH.

29  
30  
31 *Oocyte Isolation and Injection* - Capped cRNA was synthesized using a linearized cDNA template and  
32  
33 the T7 mMessage mMachine kit (Ambion). *Xenopus laevis* oocytes were isolated and dissociated using  
34  
35 collagenase as described (22) followed by injection with 50 nl of water or cRNA at 0.4 ng/nl (20  
36  
37 ng/oocyte), using a Nanoject-II injector (Drummond Scientific, Broomall, PA). Oocytes were maintained  
38  
39 at 16°C in OR3 medium (22) and studied 3-6 days after injection.

40  
41  
42 *Radioactive uptake* - Zinc uptake into oocytes was measured by incubating groups of 8-10 *X. laevis*  
43  
44 oocytes for 30 min in 1 ml of uptake buffer (ND96: 96 mM NaCl, 2 mM KCl, 1 mM MgCl<sub>2</sub>, 1.8 mM  
45  
46 CaCl<sub>2</sub>, 5 mM MES, 1 mM HEPES, 1 mM Tris<sup>6</sup>, pH 6.0) plus 100 µM ZnCl<sub>2</sub> including 0.05 µCi <sup>63</sup>Zn<sup>2+</sup>  
47  
48 (prepared as reported in ref.(23)). Oocytes were washed three times in uptake buffer plus 1 mM ZnCl<sub>2</sub>  
49  
50 before measuring <sup>63</sup>Zn<sup>2+</sup> incorporation into single oocytes as γ emission with a WIZARD2 gamma counter  
51  
52 (Perkin Elmer). For <sup>63</sup>Zn<sup>2+</sup> uptake at different pH the amounts of MES, HEPES and Tris were varied. To  
53  
54 determine the effect of HCO<sub>3</sub><sup>-</sup> on ZIP2 function 96 mM NaCl was replaced by 96 mM NaHCO<sub>3</sub> in the  
55  
56 standard ND96. In sodium replacement assays 96 mM NaCl was replaced by 96 mM choline chloride or  
57  
58 96 mM KCl.

59  
60  
61 Radioactive iron uptake experiments in HEK293 cells were performed as described earlier (20). Briefly,  
62  
63 cells were plated in 96-well, clear-bottom, white-well plates coated with poly-D-lysine at a density of 2 x  
64  
65 10<sup>4</sup> cells per well. The next day, cells were transfected with ZIP2-pIRES2 DsRed-Express2 or hDMT1-  
66  
67 pIRES2 DsRed-Express2 using lipotransfection. On the experimental day, the growth medium was  
68  
69 aspirated and cells were washed 3 times with Krebs–Ringer buffer (140 mM NaCl, 2.5 mM KCl, 1.2 mM

5 NMDG, N-Methyl-D-glucamine

6 Tris, 2-Amino-2-(hydroxymethyl) propane-1,3-diol

1  
2  
3 MgCl<sub>2</sub>, 1.2 mM CaCl<sub>2</sub>, 10 mM D-glucose, 5 mM HEPES, 5 mM MES pH = 7.4). To measure iron uptake  
4 the Krebs–Ringer buffer (pH = 5.5) was supplemented with 1 mM ascorbic acid, 1 μM FeCl<sub>2</sub> and 5  
5 μCi/ml radioactive [<sup>55</sup>Fe] iron. The assay was terminated after 15 min by washing the plates 4 times with  
6 ice cold Krebs–Ringer buffer. Subsequently, 100 μl of MicroScint-20 (PerkinElmer) were dispensed into  
7 each well and incubated at RT<sup>7</sup> for 1h under constant agitation. Radioactive [<sup>55</sup>Fe] iron uptake was  
8 measured using a TopCount Microplate Scintillation and Luminescence Counter (PerkinElmer).  
9

10  
11  
12  
13 *Two-electrode Voltage Clamp* - Two-microelectrode voltage clamping (TEVC) was used to measure  
14 steady-state currents in control oocytes and oocytes injected with ZIP2 mRNA, 4–7 days after injection.  
15 Oocyte membrane currents were recorded using an OC-725C voltage clamp (Warner Instruments,  
16 Hamden, CT), filtered at 2–5 kHz, digitized at 10 kHz, and recorded with Pulse software, and data were  
17 analysed using the PulseFit program (HEKA), as previously described (22). Voltage microelectrodes  
18 (resistance 0.5–5 MΩ) were made from fiber-capillary borosilicate and filled with 3M KCl. Oocytes were  
19 perfused at room temperature in ND96 buffer. For periods when current-voltage (*I-V*) protocols were not  
20 being run, oocytes were clamped at a holding potential (*V<sub>h</sub>*) of -60 mV. *I-V* protocols consisted of 100-ms  
21 steps-changes in membrane potential from -120 mV to +40 mV in 20-mV increments before and after the  
22 addition of the test substrate. The resulting data were filtered at 5 kHz (8 pole Bessel filter, Frequency  
23 Devices) and sampled at 1 kHz. *I-V* relationship was determined by plotting the mean steady-state current  
24 against voltage for a given set of experiments. Additionally, current was monitored continuously in  
25 oocytes clamped at *V<sub>h</sub>* -60 mV. Test solutions were perfused at room temperature for several minutes  
26 until a steady-state current was observed.  
27

28  
29  
30  
31  
32  
33  
34  
35  
36 *pH Microelectrodes* - Ion-selective microelectrodes were used to monitor intracellular pH (*pHi*) of ZIP2-  
37 and water-injected oocytes as previously described (22). Ion-selective electrodes were pulled similarly to  
38 those used for TEVC and silanized with bis-(dimethylamino)-dimethylsilane (Fluka Chemical Corp.,  
39 Ronkonkoma, NY). Electrode tips were filled with hydrogen ionophore 1-cocktail B (Fluka) and back-  
40 filled with phosphate buffer at pH 7.0. Intracellular pH was measured as the difference between the pH  
41 electrode and a KCl voltage electrode impaled into the oocyte, and membrane potential (*V<sub>m</sub>*) was the  
42 potential difference between the KCl and an extracellular calomel microelectrode. Electrodes were  
43 calibrated using pH 6.0 and 8.0 (Fisher), followed by point calibration in ND96 (pH 7.50). All pH  
44 microelectrodes used had slopes of at least -54 mV/ pH unit.  
45

46  
47  
48  
49  
50  
51 *Confocal Cd<sup>2+</sup>-flux imaging - Single cell with clamped membrane potential; patch clamping* - Membrane  
52 potential was clamped to -60 mV using the patch clamp technique in the whole-cell configuration. The  
53 pipette solution was composed of: Cs-Asp<sup>8</sup> 120 mM, TEA-Cl<sup>9</sup> 20 mM, K<sub>2</sub>ATP<sup>10</sup> 5 mM, NaCl 8 mM,  
54

55  
56  
57 <sup>7</sup> RT, Room temperature

58 <sup>8</sup> Cs-Asp, Cesium-Aspartate

1  
2  
3 MgCl<sub>2</sub> 5.6 mM (free Mg<sup>2+</sup> 0.75 mM) and HEPES 20 mM and 50 μM Fluo 3 pentapotassium salt. Note  
4 that, for this experimental set, in order to monitor Cd<sup>2+</sup> fluxes, the Calcium 5 dye was replaced by Fluo-3,  
5 another calcium indicator that is sensitive to Cd<sup>2+</sup> (24). The reason is because a membrane impermeable  
6 dye was required to avoid unspecific signal loss after cell loading. The pH was adjusted to 7.2 with CsOH  
7 and the osmolality was 285 mosmol/Kg. The external solution was composed of: NaCl 117 mM, KCl 4.8  
8 mM, MgCl<sub>2</sub> 1 mM, D-Glucose 5 mM, HEPES 5 mM and MES 5 mM. The pH was adjusted to 6.5 with  
9 1N HCl. In high potassium condition NaCl was replaced by equimolar KCl. All experiments were carried  
10 out at room temperature.  
11  
12  
13  
14  
15

16 *Confocal Cd<sup>2+</sup> imaging - Multi-cells recording* - Calcium-5 fluorescent dye (Molecular Devices) was used  
17 to record Cd<sup>2+</sup> uptake. Prior to the measurements, cells were incubated 1h at 37°C in the following  
18 external solution (in mM): NaCl 117, KCl 4.8, MgCl<sub>2</sub> 1, mM D-Glucose 10, HEPES 5, MES 5 and  
19 Calcium-5 dye). The pH was adjusted to 6.5 with HCl 1N. In high potassium condition NaCl was  
20 replaced by equimolar KCl. All experiments were carried out at room temperature.  
21  
22  
23

24 Cd<sup>2+</sup> images were acquired with a FluoView 1000 (Olympus) confocal laser-scanning microscope. Fluo-3  
25 and Calcium-5 dye were excited at 473 nm with a solid-state laser and fluorescence was detected between  
26 515 and 585 nm. To control cell transfection, DsRed-Express2 was excited at 561 nm or 488 nm with a  
27 solid-state laser and fluorescence was detected at >585 nm. Images were processed and analysed using  
28 the software ImageJ. The measurements are expressed as ΔF/F<sub>0</sub>, whereby F<sub>0</sub> is the fluorescence recorded  
29 before Cd<sup>2+</sup> application.  
30  
31  
32  
33

34 *Statistical analyses* – The normal distribution of the experimental groups was determined by  
35 Kolmogorov-Smirnov (N>50) and Shapiro-Wilk (N<50) tests. Normally distributed independent  
36 experimental groups were compared by unpaired Student's test. When not normally distributed, Mann-  
37 Whitney U test was used to assess differences. Statistical test were performed using the IBM statistics 20  
38 software. P values lower than 0.05 are considered statically significant.  
39  
40  
41  
42

## 43 **Results**

44  
45  
46  
47  
48  
49  
50  
51  
52  
53  
54  
55

---

56 <sup>9</sup> Tetraethylammonium chloride

57 <sup>10</sup> Adenosine 5'-triphosphate dipotassium salt

58  
59  
60



Dependence of ZIP2 functional activity on extracellular pH - Based on the studies of Gaither et al., the functional activity of ZIP2 was found to be inhibited at pH levels below 7.0 (1). On the other hand, our fluorescence-based transport assay using transiently transfected HEK293 cells revealed that, at acidic pH (6.5), ZIP2-mediated  $\text{Cd}^{2+}$  transport was greatly increased compared to pH 7.5 (2). What could be the reason for this discrepancy? In our assay, pH changes may have influenced the binding affinity of the fluorescent-dye used (Calcium 5) to measure  $\text{Cd}^{2+}$ . Also,  $\text{Cd}^{2+}$  rather than  $\text{Zn}^{2+}$  transport was measured which might account for the reversed pH dependence. We therefore decided to perform additional experiments to evaluate this incongruity. To this end, we used the standard radioactive tracer method using *Xenopus laevis* oocytes as an expression system, thus ensuring the same functional readout as used by Gaither et al in their studies. Using this methodology, the effect of variable extracellular pH values (pH 5.0 - 8.2) on ZIP2-mediated  $^{63}\text{Zn}^{2+}$  uptake was determined (Figure 1A). Whereas the water-injected oocytes showed only a slight pH-dependence of endogenous  $\text{Zn}^{2+}$  transport activity, ZIP2 transport activity was maximal at acidic pH <6.0 and almost negligible at pH >7.5. These results confirmed our

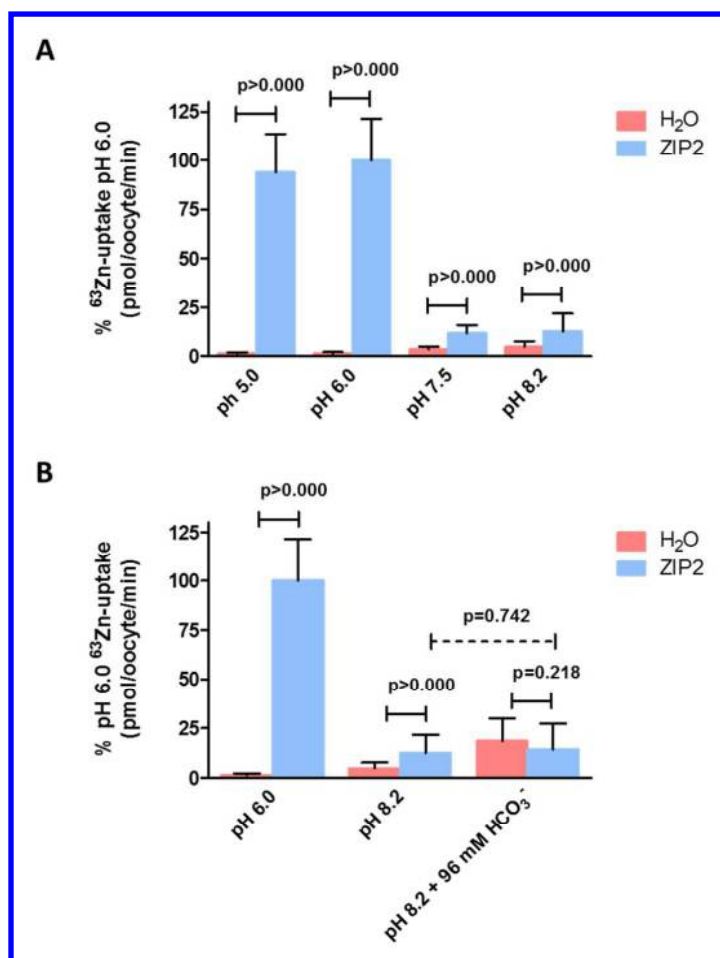


**Fig. 1. Effect of extracellular pH and bicarbonate upon  $^{63}\text{Zn}^{2+}$  uptake by ZIP2-expressing *X. laevis* oocytes.** Uptake of  $^{63}\text{Zn}^{2+}$  in the presence of 100  $\mu\text{M}$   $\text{ZnCl}_2$  by ZIP2- and  $\text{H}_2\text{O}$ -injected *X. laevis* oocytes was measured at (A) different extracellular pH (pH 5-8.2) and (B) in the absence (pH 6 and 8.2) and presence of  $\text{HCO}_3^-$  (96 mM) at pH 8.2. Data from 3 different batches of oocytes were normalized to the mean  $\text{Zn}^{2+}$  uptake by ZIP2 at pH 6.0 ( $580 \pm 124$  to  $403 \pm 62$  pmol/oocyte/min) and are represented as the Mean  $\pm$  S.D. (6 to 26 oocytes).

previous findings (2) and further validate our fluorescence assay which was used as a screening assay to identify ZIP2 modulators.

$Zn^{2+}$  transport mediated by ZIP2 is not coupled to  $HCO_3^-$  - It was previously proposed that ZIP2 operates as a  $Zn^{2+}/HCO_3^-$  cotransporter (1). We aimed to confirm this hypothesis by measuring  $^{63}Zn^{2+}$  uptake by ZIP2 cRNA<sup>11</sup> microinjected *X. laevis* oocytes in the presence and absence of  $HCO_3^-$ . To this end, we replaced the [NaCl] of the uptake solution by equimolar [NaHCO<sub>3</sub>] which resulted in a pH of 8.2. Since adjusting the pH of the solution would alter [ $HCO_3^-$ ], we compared the  $^{63}Zn^{2+}$  uptake in the  $HCO_3^-$ -containing solution with the normal uptake solution, both at pH 8.2 (Figure 1B). We did not observe a difference in the transport activity of ZIP2, whereas the H<sub>2</sub>O-injected oocytes showed a higher activity at increased [ $HCO_3^-$ ]. Additionally, in order to confirm these findings, we used pH sensitive microelectrodes

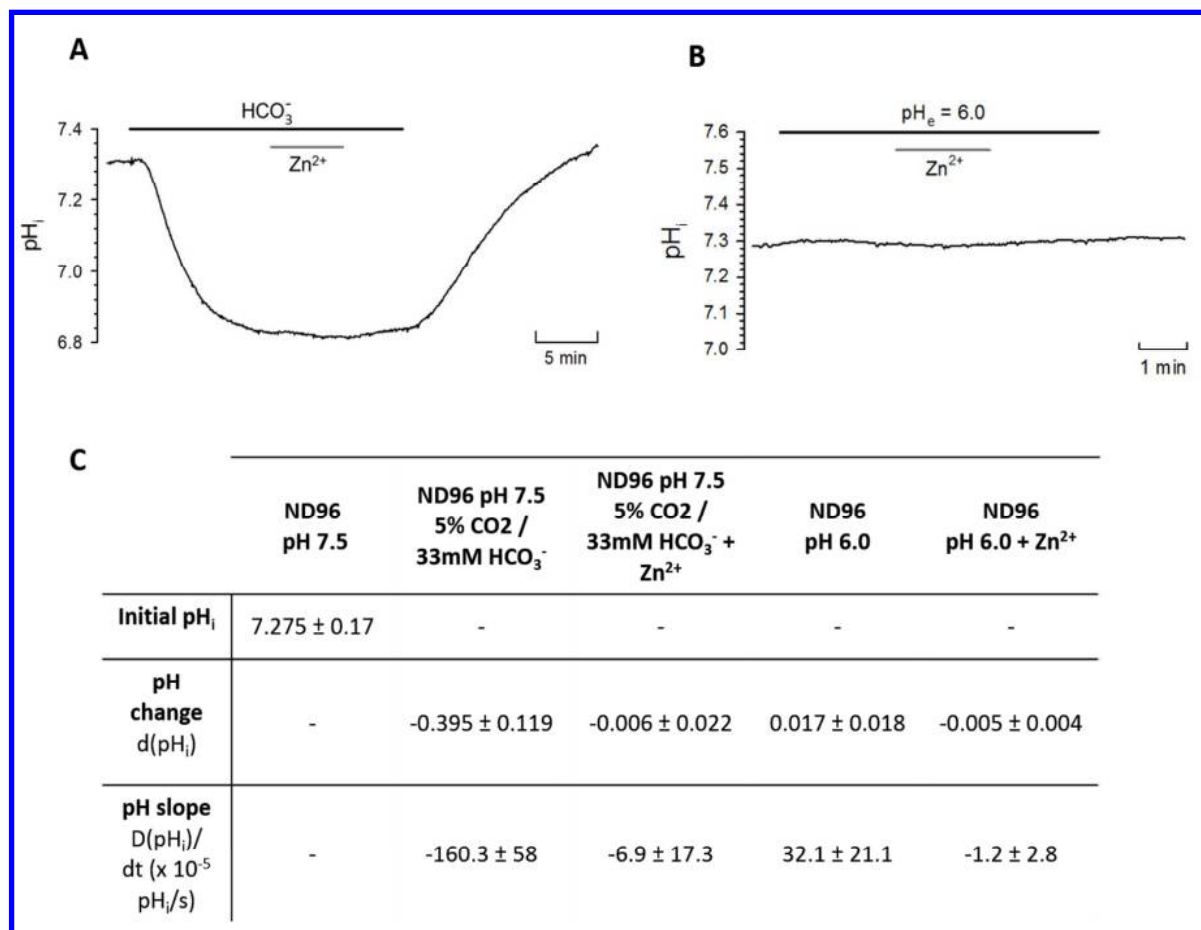


**Fig. 2 Role of bicarbonate and protons on zinc uptake by ZIP2-expressing *X.laevis* oocytes.**

Representative trace of intracellular pH (pH<sub>i</sub>) changes in response to perfusion of CO<sub>2</sub> (5%)/HCO<sub>3</sub><sup>-</sup> (33 mM) (A) or ND96 pH 6.0 (B) in the absence and presence of Zn<sup>2+</sup> (100 μM). Transport activity of ZIP2 was monitored as change in pH<sub>i</sub> when Zn<sup>2+</sup> was added and removed extracellularly. C) Summary table of the pH change and pH slope (10<sup>-5</sup> pH units/s) determined after the perfusion of each of the different media. Results are the Mean ± S.D. (2-6 oocytes).

<sup>11</sup> cRNA, complementary RNA

1  
2  
3 to measure intracellular pH ( $\text{pH}_i$ <sup>12</sup>) changes due to  $\text{HCO}_3^-$ -coupled  $\text{Zn}^{2+}$  transport via ZIP2 expressed *X.*  
4 *laevis* oocytes (Figure 2A). The uptake buffer was equilibrated by addition of 5%  $\text{CO}_2$  / 33 mM  $\text{HCO}_3^-$ .  
5 The  $\text{CO}_2$  caused an acidification in ZIP2-injected oocytes (Figure 2A and C) as well as in  $\text{H}_2\text{O}$ -injected  
6 oocytes (data not shown). Upon perfusion of  $\text{Zn}^{2+}$ , the  $\text{pH}_i$  did not change, contradictory to what would be  
7 expected if the transport was coupled to  $\text{HCO}_3^-$  (Figure 2A and C).  
8  
9

10  
11 *ZIP2 does not transport  $\text{H}^+$*  - Our experiments suggests that  $\text{H}^+$  may be involved in the ZIP2-mediated  
12 transport process. Thus, we also used the pH sensitive microelectrodes in *X. laevis* oocytes to investigate  
13 whether protons are coupled to ZIP2 mediated  $\text{Zn}^{2+}$  transport (Figure 2B). Almost no change was  
14 observed when the pH 7.5 uptake solution was replaced by pH 6 solution, indicating that there is no  $\text{H}^+$   
15 permeation via ZIP2. Also, addition of  $\text{Zn}^{2+}$  did not cause a significant change in  $\text{pH}_i$  in ZIP2-injected  
16 oocytes (Figure 2B and C). These results indicate that ZIP2 does not facilitate transport of  $\text{H}^+$ , neither  
17 alone nor coupled to  $\text{Zn}^{2+}$  transport.  
18  
19

20  
21 *ZIP2 is not electrogenic* - To test whether ZIP2-mediated  $\text{Zn}^{2+}$  transport is electrogenic, functional  
22 experiments were performed using two-electrode-voltage-clamp (TEVC<sup>13</sup>). We did not observe any  
23 discernible change in the current-voltage ( $I$ - $V$ <sup>14</sup>) relationship following step-changes in membrane  
24 potential ( $V_m$ <sup>15</sup>) of oocytes expressing ZIP2 at extracellular pH 7.5 or 6.0 (Figures 3A and B). Moreover  
25 perfusion of  $\text{Zn}^{2+}$  (100  $\mu\text{M}$ ) did not evoke any appreciable change in the  $I$ - $V$  relationship (Figures 3A and  
26 B). Similar results were obtained when current was monitored continuously in oocytes clamped ( $V_h$ <sup>16</sup>) at -  
27 60 mV (data not shown). Hence, functional experiments performed with TEVC indicate that there are no  
28 measurable currents associated with ZIP2-mediated  $\text{Zn}^{2+}$  transport which is surprising, given the positive  
29 charge of the divalent metal ion  $\text{Zn}^{2+}$  and the highly significant transport activity observed for ZIP2  
30 cRNA-injected oocytes when measuring  $^{63}\text{Zn}^{2+}$  accumulation under similar experimental conditions  
31 (Figure 1).  
32  
33  
34  
35  
36  
37  
38  
39  
40  
41  
42  
43  
44  
45  
46  
47  
48  
49  
50  
51  
52

---

53  
54 <sup>12</sup>  $\text{pH}_i$ , intracellular pH

55 <sup>13</sup> TEVC, two-electrode-voltage-clamp

56 <sup>14</sup>  $I$ - $V$ , Intensity-voltage

57 <sup>15</sup>  $V_m$ , membrane potential

58 <sup>16</sup>  $V_h$ , holding voltage

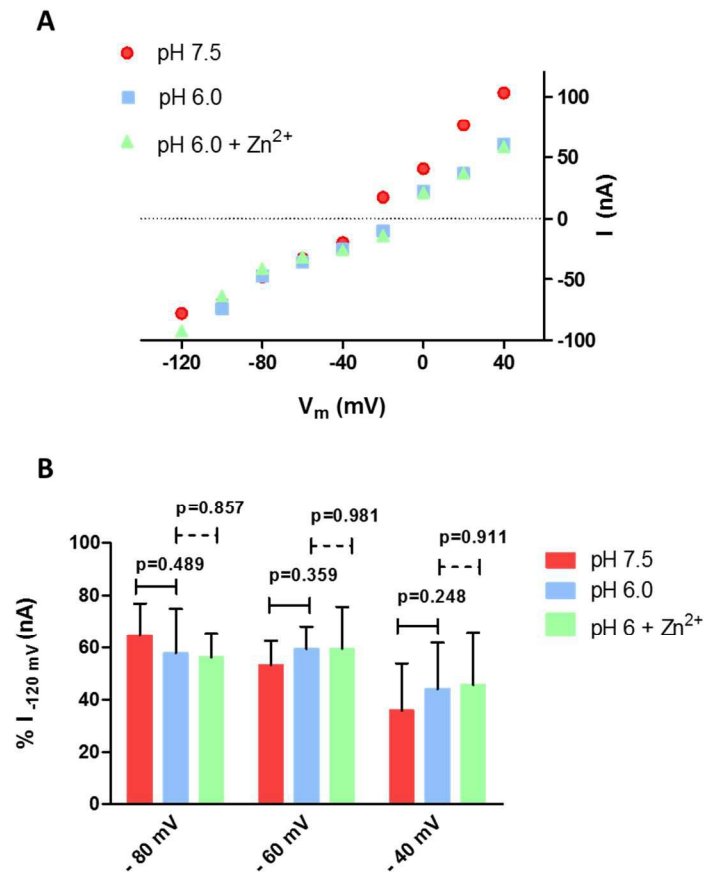


**Fig. 3. Electrophysiological properties of ZIP2-expressing *X.laevis* oocytes.** **A)** Representative trace of the current-voltage relationship under the indicated conditions ( $V_h = -60$  mV;  $100 \mu\text{M Zn}^{2+}$ ). **B)** Average currents recorded under the indicated conditions. For each individual oocyte the data were normalized to the current recorded at  $-120$  mV in pH 7.5 medium ( $-159.37$  to  $-38.75$  nA). Data from the different oocytes ( $n = 6$ ) were pooled together and are represented as the Mean  $\pm$  S.D.

Transport mediated by ZIP2 is not dependent on  $\text{Na}^+$  or  $\text{Cl}^-$  gradients, but is inhibited by  $\text{K}^+$  - We investigated whether ZIP2-mediated transport is coupled to  $\text{Na}^+$ ,  $\text{K}^+$  or  $\text{Cl}^-$ , by isosmotic replacement of these ions in the standard uptake solution. To address this question, we used both a fluorescent-based  $\text{Cd}^{2+}$  influx assay (Fig. 4A) in transiently transfected HEK293 cells and a  $^{63}\text{Zn}^{2+}$  uptake assay in ZIP2-cRNA-injected *X. laevis* oocytes (Fig. 4B).  $[\text{Na}^+]$  was replaced by equimolar [NMDG], [choline] or  $[\text{K}^+]$ , whereas  $[\text{Cl}^-]$  was replaced by the corresponding gluconate salts. Replacement of  $\text{Na}^+$  with NMDG or

choline had no effect on ZIP2 activity, whereas replacing it by  $K^+$  reduced transport by  $\approx 60$ -40 %. Replacement of chloride by gluconate salts did not have any effect on ZIP2 activity.

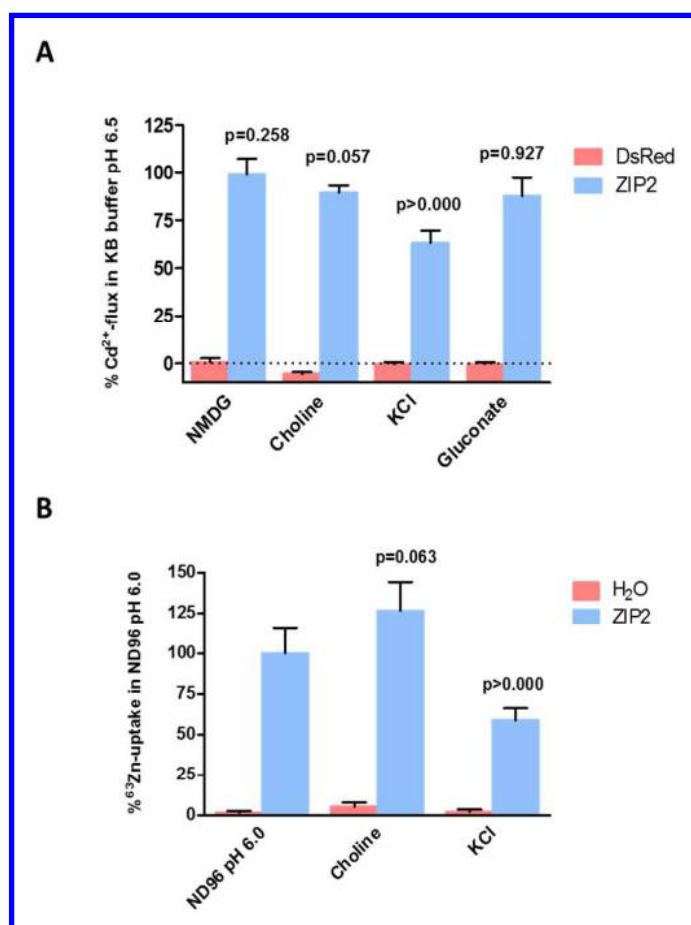


**Fig. 4. Effect of sodium, chloride and potassium extracellular concentration over ZIP2 transport activity.** A)

Changes of fluorescence intensity of Calcium-5-dye in response to  $Cd^{2+}$  perfusion ( $1 \mu M$ ) measured in HEK293 cells transiently transfected with DsRed Express2 and ZIP2 DNA constructs in KB buffer pH 6.5 in which extracellular  $[Na^+]$  or  $[Cl^-]$  were replaced by equimolar  $[NMDG]$ ,  $[Choline^+]$  and  $[K^+]$  or  $[Gluconate\ salts]$  respectively. Data from 2 independent experiments were normalized to the mean ZIP2 activity at pH 6.5 and are represented as the Mean  $\pm$  S.D. ( $n = 8-12$ ). B) Uptake of  $^{63}Zn^{2+}$  in the presence of  $100 \mu M$   $ZnCl_2$  by ZIP2- and H<sub>2</sub>O-injected *X. laevis* oocytes was measured in ND96 pH 6.0 in which extracellular  $[Na^+]$  was replaced by equimolar  $[Choline^+]$  or  $[K^+]$ . Data from 2 different batches of oocytes were normalized to the mean  $Zn^{2+}$  uptake by ZIP2 at pH 6.0 ( $403 \pm 62$  pmol/oocyte/min) and are represented as

Transport mediated by ZIP2 is not coupled to  $K^+$ , but it is voltage-dependent - To clarify whether the reduction in ZIP2-mediated  $Cd^{2+}$  or  $Zn^{2+}$  transport when replacing  $Na^+$  by  $K^+$  is due to direct  $K^+$ -coupled metal ion transport or merely a result of membrane depolarization generated by increased extracellular  $[K^+]$ , fluorometric analysis under voltage-clamp condition was conducted. First, fluorometric measurements were carried out without voltage clamping, within an open field of ZIP2 transfected cells (Fig. 5A, B and C). In line with our previous observations,  $[Na^+]$  replacement by equimolar  $[K^+]$  induced an inhibition  $\approx 40\%$  of the ZIP2-mediated influx of  $Cd^{2+}$ . Next, the same procedure was performed in individual cells under voltage-clamp conditions ( $V_h = -60$  mV) (Fig. 5D, E and F). Interestingly, under

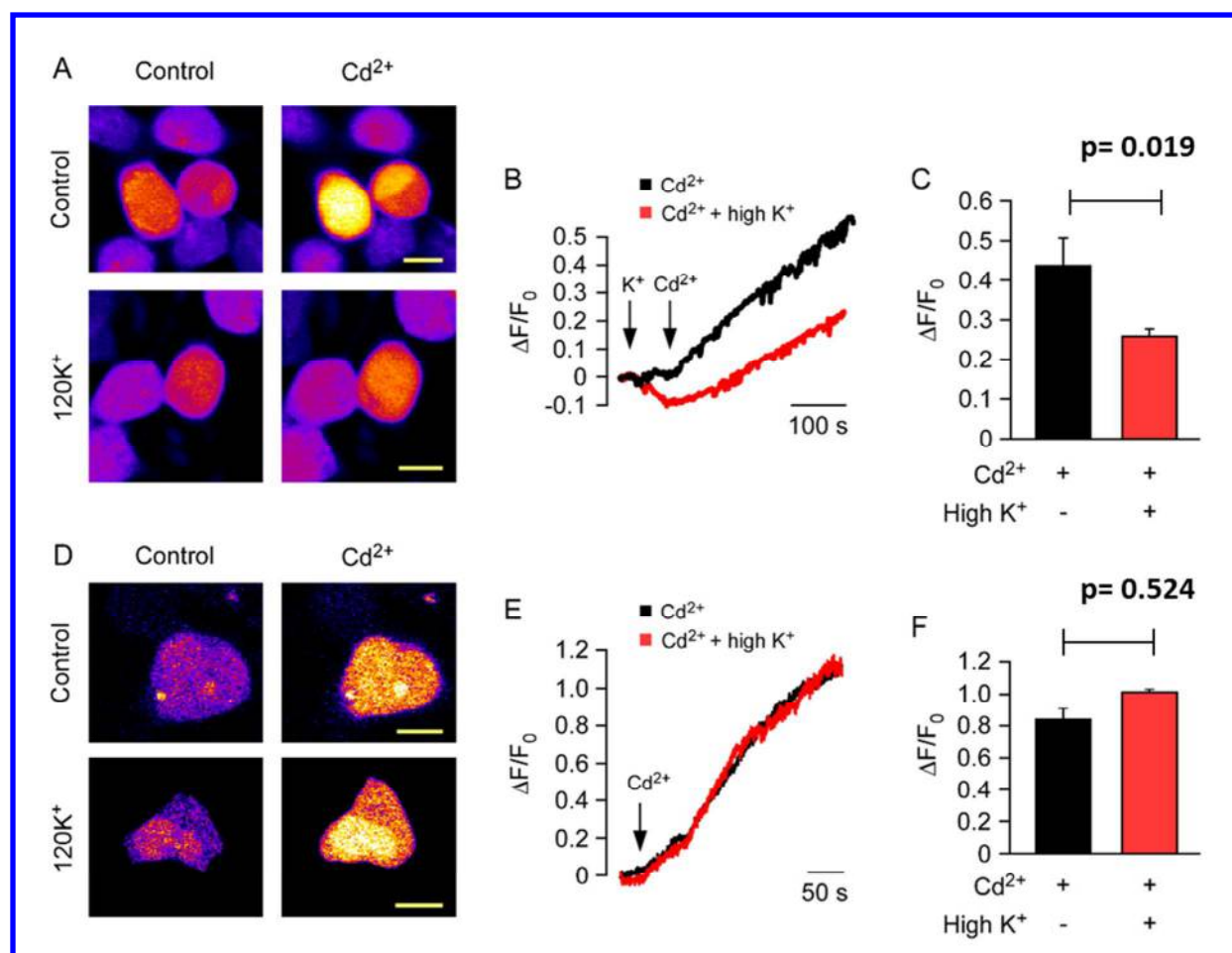


**Fig.5. Effect of potassium over membrane potential in ZIP2 transiently transfected HEK293 cells.**

Representative images of intact (A) or dialyzed (D) cells before and after the treatment with  $Cd^{2+}$  ( $10 \mu M$ ) in the presence (control) or absence of extracellular  $120$  mM  $K^+$ . Representative traces of  $Cd^{2+}$ -flux induced changes on fluorescence intensity in intact (B) and clamped (E) cells in the presence and absence of  $120$  mM  $K^+$ . Fluorescence intensity changes were measured as  $\Delta F/F_0$  (where  $F_0$  is the signal before  $Cd^{2+}$  application). Data from 3 and 5 independent experiments for intact ( $n=38-41$ ) and dialyzed ( $n= 8-10$ ) cells, respectively, were represented as Mean  $\pm$  S.D.

voltage-clamp conditions, the inhibition was lost and the ZIP2-mediated influx of  $\text{Cd}^{2+}$  was similar in the presence and absence of high extracellular  $[\text{K}^+]$ . These results demonstrate that  $\text{K}^+$  is not part of the translocation mechanism of ZIP2 and that transport is voltage-dependent.

*Transport kinetics and pH-dependence of ZIP2* - The kinetics of ZIP2-mediated transport was studied using our  $\text{Cd}^{2+}$ -flux fluorescence-based assay in transiently transfected HEK293 cells. Fluorescence

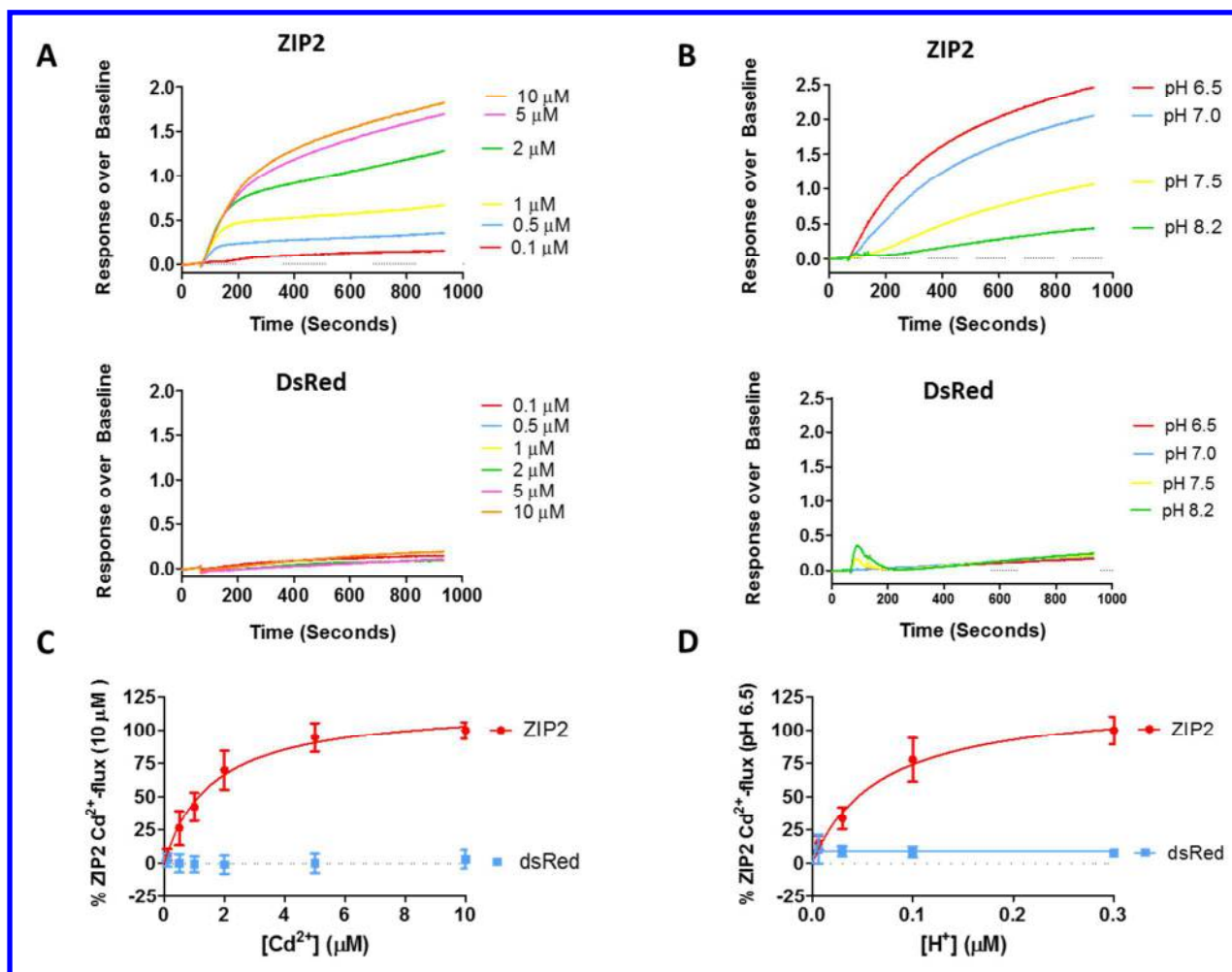


**Fig. 6. Kinetics and pH-dependence of the  $\text{Cd}^{2+}$  transport measured in ZIP2 or DsRed Express2 (empty vector) transiently transfected HEK293 cells.** Representative experiments showing the changes on fluorescence intensity of Calcium-5-dye in response to the perfusion of different  $\text{Cd}^{2+}$  concentrations (0.1-10  $\mu\text{M}$ ) at extracellular pH 6.5 (A) or at different extracellular pH values (6.5-8.2) in the presence of saturating concentration of  $\text{Cd}^{2+}$  (10  $\mu\text{M}$ ) (B). To determine the Kinetics (C) and pH-dependence (D) of  $\text{Cd}^{2+}$  transport, the Area under the curve (AUC) for each single trace was calculated. Data from 3 independent experiments were normalized to the mean  $\text{Cd}^{2+}$  uptake by ZIP2 at pH 6.5 ( $337.22 \pm 34$  to  $890 \pm 22$  AUC), collected and are represented as the mean  $\pm$  S. D. (n = 7-28). Kinetic parameters were obtained by fitting the data points to the Michaelis-Menten equation (solid lines).

intensity changes increased with extracellular  $[Cd^{2+}]$  (Fig.6A; upper panel). Measuring  $Cd^{2+}$ -flux through ZIP2 gave a dose-response curve that saturated at  $5 \mu M [Cd^{2+}]$  (Fig. 6C). The calculated apparent affinity constant  $K_m$  for  $Cd^{2+}$  was  $\sim 1.57 \pm 0.18 \mu M$ . Empty-vector transfected cells did not show any change in fluorescent intensity within the range of  $[Cd^{2+}]$  tested (Fig.6A; lower panel).

Using the same methodology, the pH-dependence of the ZIP2-mediated transport was studied. In line with our previous findings, fluorescent intensity changes after  $Cd^{2+}$  ( $10 \mu M$ ) perfusion increased with the extracellular  $[H^+]$  (Fig.6B; upper panel). Transport was completely saturated at extracellular pH 6.5 and the calculated apparent affinity was  $K_{H^+} \sim 66 \pm 16 \text{ nM}$ , corresponding to pH  $\sim 7.2$  (Fig.6C). Again, no effect was observed over the empty-vector transfected cells (Fig.6B; lower panel).

*Cation selectivity of ZIP2* - In order to investigate the cationic selectivity of ZIP2,  $Cd^{2+}$ -flux was measured in the presence of high extracellular concentrations ( $50 \mu M$ ) of different divalent cations such as  $Ba^{2+}$ ,  $Mn^{2+}$ ,  $Co^{2+}$ ,  $Zn^{2+}$  and  $Cu^{2+}$  (Fig. 7A). Note that none of these metal ions showed significant interactions with the Calcium 5 dye when high concentrations of them ( $100 \mu M$ ) were perfused individually into ZIP2 overexpressing cells (data not shown). As expected, in the presence of  $Zn^{2+}$ ,  $Cd^{2+}$ -flux was completely inhibited. Interestingly,  $Cu^{2+}$  and  $Co^{2+}$  inhibited 75% and 25%, respectively, of the  $Cd^{2+}$ -flux, while no significant inhibition was observed by  $Ba^{2+}$  or  $Mn^{2+}$ .  $Fe^{2+}$  is another putative substrate of ZIP2. However, since it also interacts with the  $Ca^{2+}$ -5-dye, it was not included in this set of experiments. To overcome this issue, we measured directly the radiolabeled iron ( $^{55}Fe^{2+}$ ) uptake (Fig. 7B). As a positive control for this assay, we used the human divalent metal transporter 1 (hDMT1, SLC11A2) (25).  $^{55}Fe^{2+}$ -uptake by ZIP2 was not significantly different from that of empty vector-transfected cells and 7-fold lower than the uptake mediated by hDMT1, demonstrating that  $Fe^{2+}$  is not substrate of ZIP2.

To determine the apparent affinity of ZIP2 for  $Zn^{2+}$  and  $Cu^{2+}$ ,  $Cd^{2+}$ -flux was measured in the presence of a range of extracellular concentrations of  $Zn^{2+}$  or  $Cu^{2+}$ . In both cases, inhibition of  $Cd^{2+}$ -flux gave dose-response sigmoidal curves. The calculated  $IC_{50}$  values were  $\sim 0.52 \pm 1.7 \mu M$  for  $Zn^{2+}$  (Fig. 7C) and  $\sim 2.98 \pm 1.3 \mu M$  for  $Cu^{2+}$  (Fig. 7D). Given that the  $K_m$  of ZIP2 for  $Cd^{2+}$  is  $1.57 \mu M$  (Fig. 6C), according to the Cheng-Prusoff equation (26), the  $IC_{50}$  values for  $Zn^{2+}$  and  $Cu^{2+}$  are  $0.32 \mu M$  and  $1.81 \mu M$  respectively. Hence, the cationic selectivity for ZIP2 decreases in the order  $Zn^{2+} > Cd^{2+} \geq Cu^{2+} > Co^{2+}$ , while  $Fe^{2+}$ ,  $Mn^{2+}$  and  $Ba^{2+}$  are not transport substrates.



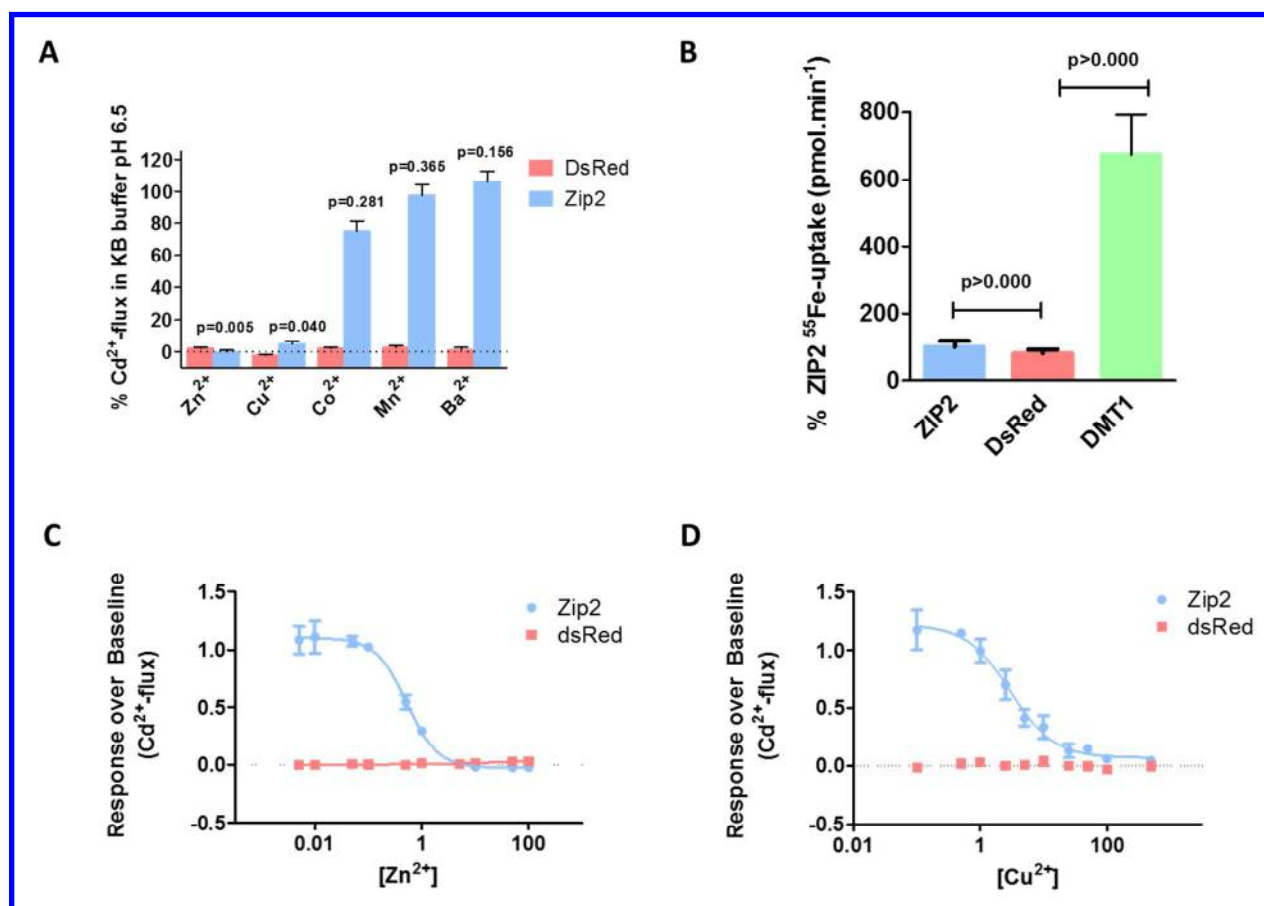


**Fig. 7. Divalent cation selectivity of ZIP2 in transiently transfected HEK293 cells.** **A)** Changes of fluorescence intensity of Calcium-5-dye in response to Cd<sup>2+</sup> perfusion (1  $\mu$ M) measured in the presence of the indicated divalent cations (50  $\mu$ M) at pH 6.5. Data from 2 independent experiments were normalized to the mean ZIP2 activity at pH 6.5 in the absence of divalent cations other than Cd<sup>2+</sup> (1 $\mu$ M) and are represented as the mean  $\pm$  S.D. (n = 5-8). P-values establish statistical differences between ZIP2 mediated Cd<sup>2+</sup>-uptake in the absence *Vs* the presence of the indicated divalent metals **B)** Uptake of <sup>55</sup>Fe<sup>2+</sup> in the presence of 1  $\mu$ M FeCl<sub>2</sub> and 100  $\mu$ M Ascorbic Acid by HK293 cells transiently transfected with ZIP2, DsRed Express2 (empty vector) and DMT1 DNA constructs at extracellular pH 5.5. Data from 2 independent experiment were normalized to the mean ZIP2 <sup>55</sup>Fe<sup>2+</sup> transport (0.09  $\pm$  0.01 to 0.15  $\pm$  0.02 pmol.min<sup>-1</sup>) and represented as the mean  $\pm$  S.D. (n =19-48). Inhibition of the ZIP2-mediated Cd<sup>2+</sup> transport (1  $\mu$ M) by increasing extracellular [Zn<sup>2+</sup>] (**C**) and [Cu<sup>2+</sup>] (**D**). Data from 2 independent experiments were normalized to the mean ZIP2 activity at pH 6.5 in the absence of divalent cations other than Cd<sup>2+</sup> and are represented as the mean  $\pm$  S.D. (n = 7). Inhibitory kinetics were obtained by fitting the data points to a 4-parameter sigmoidal equation (solid lines).

## Discussion

1  
2  
3 In our functional experiments using different approaches, ZIP2-mediated transport was increased at acidic  
4 pH, even though no cotransport with  $H^+$  was observed. We therefore conclude that the ZIP2 transport  
5 process is modulated by extracellular pH, independent of the  $H^+$  driving force. Transport was not  
6 stimulated by the presence of  $HCO_3^-$ , as previously reported (1). Thus, we conclude that ZIP2-mediated  
7 transport is not coupled to bicarbonate. Also, in contrast to the previous observations (1), our experiments  
8 revealed that increasing extracellular  $[K^+]$  inhibits ZIP2-mediated metal ion uptake under non-voltage  
9 clamp condition. However, when the  $K^+$  inhibitory effect was measured under voltage-clamp condition, it  
10 was abolished. This indicates that the inhibitory effect was due to the depolarization caused by increasing  
11 extracellular  $K^+$  concentration to 140 mM. Therefore, we concluded that ZIP2-mediated metal ion  
12 transport is voltage dependent and, given the positive charge of  $Zn^{2+}$ , we expected that transport would be  
13 electrogenic.  
14

15  
16 Paradoxically, our electrophysiological analysis revealed that ZIP2-mediated  $Zn^{2+}$  transport is  
17 electroneutral. The electrophysiological experiments were done with ZIP2 overexpressed in *X. laevis*  
18 oocytes and in the presence of a robust inwardly directed electrochemical  $Zn^{2+}$  gradient, favouring  
19 transmembrane influx (i.e. membrane voltage was kept constant at -60mV and 100  $\mu$ M  $ZnCl_2$  was  
20 perfused). Using the same experimental approach, our group observed prominent transmembrane inward  
21 currents for  $Fe^{2+}$  transport via DMT1 expressed in *X. laevis* oocytes, even at neutral pH (that is in the  
22 absence of an inwardly directed  $H^+$ -gradient) (27). Given that ZIP2 injected oocytes exhibited high  $^{63}Zn$   
23 accumulation as shown in Figure 1, this rules out any issue related to plasma membrane expression. To  
24 explain the lack of electrogenicity, we propose the following:  
25

- 26 1. Transport is still electrogenic but the turn-over rate of the transport process is too slow to  
27 allow any detection of transport-associated currents.
- 28 2. Transport is electroneutral because there is and as yet unidentified coupling ion (via  
29 cotransport or exchange) that balances the positive charges of  $Zn^{2+}$ . In this case, given the  
30 voltage dependence of the transport process, the transport cycle must contain steps that  
31 are limited by the membrane potential.  
32

33  
34 Interestingly, the transport features of ZIP2 resemble those of a ZIP transporter from the Gram-negative,  
35 rod-shaped bacterium *Bordetella bronchiseptica* (ZIPB<sup>17</sup>) (28). In that work, ZIPB was described as a  
36 selective electrodiffusional channel, in which  $Zn^{2+}$  uptake is driven only down its concentration gradient.  
37 Remarkably,  $Zn^{2+}$  transport by ZIPB was modulated by the effect of  $K^+$  on the resting membrane  
38 potential, indicating that ZIPB is also voltage-dependent. Furthermore, ZIPB-mediated  $Zn^{2+}$ -flux was  
39 modulated by pH and not stimulated by  $HCO_3^-$ . Also in line with our findings, *Fugu* pufferfish ZIP2,  
40 sharing 30% and 60% sequence identity with human ZIP2 and ZIP3, respectively, exhibited, when  
41

42  
43  
44  
45  
46  
47  
48  
49  
50  
51  
52  
53  
54  
55  
56  
57 <sup>17</sup> ZIPB, *Bordetella bronchiseptica* ZrT/Irt-like protein  
58  
59  
60

1  
2  
3 expressed in MDCK<sup>18</sup> cells, Zn<sup>2+</sup>-mediated transport in a pH-dependent manner. Transport was stimulated  
4 by acidic pH medium (pH 5.5-6.5) but was not enhanced (but rather slightly inhibited) by the presence of  
5 extracellular HCO<sub>3</sub><sup>-</sup> (29).  
6  
7

8 Altogether, given that ZIP2-mediated transport is ATP-independent (1) and not coupled to Na<sup>+</sup>, H<sup>+</sup>, K<sup>+</sup>,  
9 HCO<sub>3</sub><sup>-</sup> or Cl<sup>-</sup>, we propose that Zn<sup>2+</sup> uptake occurs via simple passive transport. Given that Zn<sup>2+</sup> is a trace  
10 element essential for most mammalian cells, efficient uptake mechanisms must exist to allow cells to  
11 accumulate Zn<sup>2+</sup>. Because intracellular Zn<sup>2+</sup> is complexed with specific binding proteins, cytoplasmic  
12 Zn<sup>2+</sup> concentrations are kept at very low (femtomolar to picomolar) levels. Consequently, the inwardly  
13 directed electrochemical Zn<sup>2+</sup> gradient is expected to be sufficient to facilitate cellular Zn<sup>2+</sup> uptake,  
14 supporting this concept of passive ZIP2-mediated transport (28).  
15  
16  
17  
18

19 The only ion showing interaction with the transport process mediated by ZIP2 is H<sup>+</sup>. Our results show  
20 that, at low extracellular pH, transport of Zn<sup>2+</sup> is increased. However, H<sup>+</sup> was not cotransported with Zn<sup>2+</sup>  
21 and there was transport at pH >7.5, indicating that ZIP2-mediated transport is modulated by pH, rather  
22 than H<sup>+</sup> acting as a coupling ion. In addition to the aforementioned ZIPB and *Fugu* pufferfish ZIP2, there  
23 are many examples of ion channels that can be modulated by external pH, including Cl<sup>-</sup> channels (30),  
24 Na<sup>+</sup> channels (31) and aquaporins (32), among others (33). In these channels, the protonation state of  
25 specific titratable residues affects voltage-dependence or gate-opening, leading to modulation of channel  
26 permeation. Future structure-function studies of ZIP2 to identify amino acidic residues responsible for  
27 H<sup>+</sup>-sensitivity will shed further light on this pH modulatory mechanism.  
28  
29  
30  
31  
32  
33

34 As described previously, ZIP2 expression has been found in prostate epithelial cells (34), peripheral blood  
35 mononuclear cells of patients with tuberculosis and asthma (5) and epidermal keratinocytes (4).  
36 Interestingly, these tissues/cell types are involved in physiological processes occurring under an acidic  
37 environment. The main function of the prostate is to secrete prostatic fluid, which is acidic (6.5-6.7)  
38 (34,35). Based on its apical membrane localization, ZIP2 is hypothesized to help maintain prostate Zn<sup>2+</sup>  
39 homeostasis by reabsorbing Zn<sup>2+</sup> from the prostatic fluid. (3). Similarly, acidification of the airways  
40 linked to different pathological processes, including inflammation, ischaemia or aspiration of refluxing  
41 gastric contents, and obstructive airway diseases such as asthma, may lead to increased ZIP2-mediated  
42 transport (33). ZIP2 expression has been described in the epidermis and, moreover, transporter-mediated  
43 Zn<sup>2+</sup> uptake is necessary for the differentiation of keratinocytes (4). The surface of healthy skin has a pH  
44 oscillating between 4.0 and 6.0 (36). Altogether, these findings further support the role of H<sup>+</sup> on the  
45 transport processes mediated by ZIP2 since, as our functional experiments point out, the functional  
46 activity of ZIP2 will be increased in these acidic environments. In turn, it seems counterintuitive to use  
47 HCO<sub>3</sub><sup>-</sup> as driving force for the transport of Zn<sup>2+</sup> under such physiological conditions as, at reduced pH, a  
48  
49  
50  
51  
52  
53  
54  
55  
56

57 <sup>18</sup> MDCK, Madin-Darby Canine Kidney cells  
58  
59  
60

1  
2  
3 significant part of bicarbonate will be in the conjugated acid form carbonic acid ( $\text{H}_2\text{CO}_3$ ) ( $\text{pK}_a = 6.2$  at  
4  $37^\circ\text{C}$ ). In this regard, upregulation of ZIP2 expression in peripheral blood mononuclear cells of patients  
5 with tuberculosis was accompanied by down-regulation of the expression of SLC39A8 (ZIP8), and the  
6 authors proposed that this could be a consequence of changes in the pH and  $\text{Zn}^{2+}$  concentrations (5).  
7 These findings suggest a complementary function of ZIP2 and ZIP8. In line with this, our preliminary  
8 experiments using the herein described fluorescent based-assay, revealed opposite pH modulation for  
9 ZIP8 compared to ZIP2 (data not shown).  
10  
11  
12  
13

14 With respect to the kinetic properties of ZIP2, our experiments indicate that the  $K_m$  for ZIP2-mediated  
15  $\text{Cd}^{2+}$  flux was  $\sim 1.6 \mu\text{M}$ , similar to that reported by Gaither and Eide for  $\text{Zn}^{2+}$  ( $K_m \sim 3 \mu\text{M}$ ) (1). On the  
16 other hand, based on our assay, ZIP2-mediated transport reached  $V_{\text{max}}$  already at  $5 \mu\text{M}$   $\text{Cd}^{2+}$  whereas in  
17 the study of Gaither *et. al.*,  $V_{\text{max}}$  for  $\text{Zn}^{2+}$  transport was  $20\text{-}40 \mu\text{M}$  (1). Another difference between the  
18 two studies exists when comparing the divalent metal competition experiments. According to our  
19 experiments, ZIP2 can transport  $\text{Zn}^{2+}$  and  $\text{Cd}^{2+}$  but not  $\text{Fe}^{2+}$ , and  $\text{Cu}^{2+}$  and  $\text{Co}^{2+}$  are likely also substrates,  
20 while  $\text{Ba}^{2+}$  and  $\text{Mn}^{2+}$  were not transported by ZIP2. In contrast, Gaither *et al.* proposed that all of these  
21 metals ions could serve as substrates of ZIP2 (1). In line with our findings, studies with HEK293 cells  
22 overexpressing mouse ZIP2, showed similar Michaelis-Menten kinetics for  $\text{Zn}^{2+}$  ( $K_m \sim 1.6 \mu\text{M}$ ) (37).  
23 Moreover,  $\text{Zn}^{2+}$  transport was inhibited in this study by excess of  $\text{Cu}^{2+}$ ,  $\text{Cd}^{2+}$ ,  $\text{Co}^{2+}$ , but not  $\text{Fe}^{2+}$  or  $\text{Mn}^{2+}$ .  
24 In contrast, the previously mentioned pufferfish ZIP2 exhibited ten-fold lower affinity for  $\text{Zn}^{2+}$  ( $K_m \sim 13$   
25  $\mu\text{M}$ ), while  $\text{Zn}^{2+}$  transport was inhibited by  $\text{Cu}^{2+}$ ,  $\text{Cd}^{2+}$ ,  $\text{Co}^{2+}$ ,  $\text{Fe}^{3+}$  and to lower extend by  $\text{Fe}^{2+}$  (29). This  
26 variabilities among competition experiments highlights the importance of determining the substrate  
27 selectivity of transporters by direct measurements of each putative substrate. In this regard, direct  
28 measurements of  $^{63}\text{Zn}$  (Figure 1 and 4B),  $\text{Cd}^{2+}$  (Figure 6) and  $^{55}\text{Fe}$  uptake (Figure 7B) confirm that  $\text{Zn}^{2+}$   
29 and  $\text{Cd}^{2+}$  are real substrates of ZIP2, while iron was not found to be a substrate. Regarding to the other  
30 proposed ZIP2 substrates (i.e.  $\text{Cu}^{2+}$  and  $\text{Co}^{2+}$ ), direct measurements will be required as well to verify them  
31 as transport substrates.  
32  
33  
34  
35  
36  
37  
38  
39  
40  
41  
42

43 The incongruities between the current work and that of Gaither *et. al.* are likely due to the use of different  
44 expression systems. Gaither *et. al.* used the chronic myeloid leukaemia cell line K562 for their  
45 radiolabelled  $\text{Zn}^{2+}$ -uptake experiments. These cells endogenously express  $\text{Zn}^{2+}$  transporters, as well as the  
46 sodium-proton exchanger NHE1 (SLC9A1) (38) and the chloride/bicarbonate anion exchanger AE2  
47 (SLC4A2) (39). Thus, the reported  $\text{Zn}^{2+}$  transport activities and divalent metal ion specificities in K652  
48 cells represent the sum of both endogenous and expressed ZIP2 transporters. In addition, the inverse pH-  
49 sensitivity and role of bicarbonate in ZIP2-mediated transport could be related to interfering activities of  
50 NHE1 and AE2. Our functional experiments were conducted in HEK293 cells, which express endogenous  
51 NHE3 (SLC9A1) (40) but not AE2 (41). Also, experiments were done in *Xenopus* oocytes, which express  
52  
53  
54  
55  
56  
57  
58  
59  
60

1  
2  
3 an NHE exchanger homolog but not any endogenous anionic exchangers (42). As functional readouts, we  
4 used a combination of different methods, including electrophysiological measurements, radiolabelled  
5  $Zn^{2+}$ -uptake experiments in *X.laevis* oocytes and  $Cd^{2+}$ -flux based fluorescent assay in HEK293 cells.  
6 Importantly, in non-injected control oocytes or in empty-vector transfected HEK cells, endogenous  $Zn^{2+}$ -  
7 transport (Figure 1) or  $Cd^{2+}$ -transport (Figure 6A) was negligible compared to ZIP2 expressing oocytes or  
8 cells. Hence, our experimental approaches guarantee an optimal signal-to-noise ratio for studying  
9 different aspects of the ZIP2 transport mechanism. This allowed us to validate our observations using  
10 different techniques, thereby generating data with great consistency, as demonstrated, for example, for the  
11 pH-dependence (Figures 1A and 6B) or the effect of  $K^+$  (Figures 4 and 5).

12  
13  
14 We anticipate that the herein reported data are valuable to predict the putative roles of ZIP2 in  
15 pathological situations or during physiological challenges. Indeed, human genetic studies revealed that  
16 ZIP2 polymorphisms constitute a risk factor for a wide variety of human diseases, including carotid artery  
17 disease in aging (43), arsenic-related bladder cancer (44) and cystic fibrosis (45). In addition, ZIP2  
18 activity is important for prostate function and related to prostate cancer development (3,34), keratinocyte  
19 differentiation (4) and macrophage (46) and monocyte function (13). Also ZIP2 knockout mice studies  
20 revealed increased susceptibility to Zn-deficiency during pregnancy (19). As a follow-up, specific  
21 experiments are needed to unveil the particular roles of ZIP2 in physiologically relevant environments.  
22 For example, functional studies with the aforementioned genetic variants will be required to reveal the  
23 precise molecular mechanisms leading to the associated disease conditions. Also, tissue specific knockout  
24 studies in cellular or animal models are required to describe the physiological and pathological impacts of  
25 ZIP2 dysfunction. Such studies may in turn accelerate the discovery of therapeutic applications targeting  
26 ZIP2.

## 27 28 29 30 31 32 33 34 35 36 37 38 39 **Conclusion**

40  
41 Our data show that ZIP2-mediated transport is modulated by extracellular pH, in an  $H^+$  driving-force  
42 independent and voltage-dependent manner. Accordingly, we propose that ZIP2 is a facilitative  
43 transporter that mediates transport of  $Zn^{2+}$  down its concentration gradient, which can be modulated by  
44 interaction of  $H^+$  with titratable acidic amino acid residues within the ZIP2 protein. Specifically, we  
45 propose that protonation of such a titratable amino acid stabilizes the ZIP2 protein in a conformation in  
46 which substrate transport is more favourable. This would explain why the transport rate is increased in the  
47 presence of  $H^+$ . ZIP2 is expressed in acidic environments, where this regulatory mechanism is expected to  
48 be important to speed up and determine the direction of the transport process.

49  
50  
51 The herein proposed transport mechanism is consistent with those of ZIPs from lower organism (i.e. ZIPB  
52 and pufferfish ZIP2) (28,29). Nevertheless, this does not necessarily hold true for all the ZIP members, as  
53 some of them have been postulated to possess different transport mechanisms. For example, ZIP8 and  
54  
55  
56  
57  
58  
59  
60

ZIP14 are described as metal/bicarbonate symporters (47,48). In this regard, as mentioned previously, preliminary experiment from our laboratory, monitoring Cd<sup>2+</sup>-fluxes through human ZIP8 overexpressing cells, showed that the activity of this transporter is not stimulated by extracellular H<sup>+</sup>, indicating a transport mechanism that is different from the herein described for ZIP2. This highlights the need for future studies for each ZIP family member individually, in order to reveal their particular transport mechanisms and to understand their distinctive contributions towards body Zn<sup>2+</sup> homeostasis.

### Acknowledgements

The authors would like to highlight and thank Tamara Locher and Yvonne Amrein for their dedication and technical support. J.P.G. was funded by the Marie Curie Actions International Fellowship Program (IFP) TransCure ([www.nccr-transcure.ch](http://www.nccr-transcure.ch)).

### References

1. Gaither, L. A., and Eide, D. J. (2000) Functional expression of the human hZIP2 zinc transporter. *J Biol Chem* **275**, 5560-5564
2. Franz, M. C., Simonin, A., Graeter, S., Hediger, M. A., and Kovacs, G. (2014) Development of the First Fluorescence Screening Assay for the SLC39A2 Zinc Transporter. *J Biomol Screen* **19**, 909-916
3. Desouki, M. M., Geradts, J., Milon, B., Franklin, R. B., and Costello, L. C. (2007) hZip2 and hZip3 zinc transporters are down regulated in human prostate adenocarcinomatous glands. *Mol Cancer* **6**, 37
4. Inoue, Y., Hasegawa, S., Ban, S., Yamada, T., Date, Y., Mizutani, H., Nakata, S., Tanaka, M., and Hirashima, N. (2014) ZIP2 protein, a zinc transporter, is associated with keratinocyte differentiation. *J Biol Chem* **289**, 21451-21462
5. Tao, Y. T., Huang, Q., Jiang, Y. L., Wang, X. L., Sun, P., Tian, Y., Wu, H. L., Zhang, M., Meng, S. B., Wang, Y. S., Sun, Q., and Zhang, L. Y. (2013) Up-regulation of Slc39A2(Zip2) mRNA in peripheral blood mononuclear cells from patients with pulmonary tuberculosis. *Mol Biol Rep* **40**, 4979-4984
6. Andreini, C., Banci, L., Bertini, I., and Rosato, A. (2006) Counting the zinc-proteins encoded in the human genome. *J Proteome Res* **5**, 196-201
7. Maret, W., and Li, Y. (2009) Coordination dynamics of zinc in proteins. *Chemical reviews* **109**, 4682-4707
8. Brown, K. H., Peerson, J. M., Rivera, J., and Allen, L. H. (2002) Effect of supplemental zinc on the growth and serum zinc concentrations of prepubertal children: a meta-analysis of randomized controlled trials. *Am J Clin Nutr* **75**, 1062-1071
9. Eide, D. J. (2006) Zinc transporters and the cellular trafficking of zinc. *Biochim Biophys Acta* **1763**, 711-722
10. Palmiter, R. D., and Huang, L. (2004) Efflux and compartmentalization of zinc by members of the SLC30 family of solute carriers. *Pflugers Arch* **447**, 744-751
11. Jeong, J., and Eide, D. J. (2013) The SLC39 family of zinc transporters. *Molecular Aspects of Medicine* **34**, 612-619
12. Liuzzi, J. P., and Cousins, R. J. (2004) Mammalian zinc transporters. *Annu Rev Nutr* **24**, 151-172
13. Cao, J., Bobo, J. A., Liuzzi, J. P., and Cousins, R. J. (2001) Effects of intracellular zinc depletion on metallothionein and ZIP2 transporter expression and apoptosis. *J Leukoc Biol* **70**, 559-566

14. Rishi, I., Baidouri, H., Abbasi, J. A., Bullard-Dillard, R., Kajdacsy-Balla, A., Pestaner, J. P., Skacel, M., Tubbs, R., and Bagasra, O. (2003) Prostate cancer in African American men is associated with downregulation of zinc transporters. *Appl Immunohistochem Mol Morphol* **11**, 253-260
15. Franz, M. C., Anderle, P., Bürzle, M., Suzuki, Y., Freeman, M. R., Hediger, M. A., and Kovacs, G. (2013) Zinc transporters in prostate cancer. *Molecular Aspects of Medicine* **34**, 735-741
16. Costello, L. C., Franklin, R. B., Zou, J., Feng, P., Bok, R., Mark, G. S., and Kurhanewicz, J. (2011) Human prostate cancer ZIP1/zinc/citrate genetic/metabolic relationship in the TRAMP prostate cancer animal model. *Cancer Biol Ther* **12**
17. Franklin, R. B., Feng, P., Milon, B., Desouki, M. M., Singh, K. K., Kajdacsy-Balla, A., Bagasra, O., and Costello, L. C. (2005) hZIP1 zinc uptake transporter down regulation and zinc depletion in prostate cancer. *Mol Cancer* **4**, 32
18. Johnson, L. A., Kanak, M. A., Kajdacsy-Balla, A., Pestaner, J. P., and Bagasra, O. (2010) Differential zinc accumulation and expression of human zinc transporter 1 (hZIP1) in prostate glands. *Methods* **52**, 316-321
19. Hara, T., Takeda, T. A., Takagishi, T., Fukue, K., Kambe, T., and Fukada, T. (2017) Physiological roles of zinc transporters: molecular and genetic importance in zinc homeostasis. *J Physiol Sci* **67**, 283-301
20. Montalbetti, N., Simonin, A., Dalghi, M. G., Kovacs, G., and Hediger, M. A. (2014) Development and Validation of a Fast and Homogeneous Cell-Based Fluorescence Screening Assay for Divalent Metal Transporter 1 (DMT1/SLC11A2) Using the FLIPR Tetra. *J Biomol Screen* **19**, 900-908
21. Kovacs, G., Montalbetti, N., Simonin, A., Danko, T., Balazs, B., Zsembery, A., and Hediger, M. A. (2012) Inhibition of the human epithelial calcium channel TRPV6 by 2-aminoethoxydiphenyl borate (2-APB). *Cell Calcium* **52**, 468-480
22. Romero, M. F., Fong, P., Berger, U. V., Hediger, M. A., and Boron, W. F. (1998) Cloning and functional expression of rNBC, an electrogenic Na(+)-HCO<sub>3</sub><sup>-</sup> cotransporter from rat kidney. *Am J Physiol* **274**, F425-432
23. DeGrado, T. R., Pandey, M. K., Byrne, J. F., Engelbrecht, H. P., Jiang, H., Packard, A. B., Thomas, K. A., Jacobson, M. S., Curran, G. L., and Lowe, V. J. (2014) Preparation and preliminary evaluation of <sup>63</sup>Zn-zinc citrate as a novel PET imaging biomarker for zinc. *J Nucl Med* **55**, 1348-1354
24. Oyama, Y., Arata, T., Chikahisa, L., Soeda, F., and Takahama, K. (2002) Estimation of increased concentration of intracellular Cd(2+) by fluo-3 in rat thymocytes exposed to CdCl<sub>2</sub>. *Environ Toxicol Pharmacol* **11**, 111-118
25. Pujol-Gimenez, J., Hediger, M. A., and Gyimesi, G. (2017) A novel proton transfer mechanism in the SLC11 family of divalent metal ion transporters. *Sci Rep* **7**, 6194
26. Cheng, Y., and Prusoff, W. H. (1973) Relationship between the inhibition constant (K<sub>1</sub>) and the concentration of inhibitor which causes 50 per cent inhibition (I<sub>50</sub>) of an enzymatic reaction. *Biochem Pharmacol* **22**, 3099-3108
27. Mackenzie, B., Ujwal, M. L., Chang, M. H., Romero, M. F., and Hediger, M. A. (2006) Divalent metal-ion transporter DMT1 mediates both H<sup>+</sup>-coupled Fe<sup>2+</sup> transport and uncoupled fluxes. *Pflugers Arch* **451**, 544-558
28. Lin, W., Chai, J., Love, J., and Fu, D. (2010) Selective electrodiffusion of zinc ions in a Zrt-, Irt-like protein, ZIPB. *J Biol Chem* **285**, 39013-39020
29. Qiu, A., and Hogstrand, C. (2005) Functional expression of a low-affinity zinc uptake transporter (FrZIP2) from pufferfish (Takifugu rubripes) in MDCK cells. *Biochem J* **390**, 777-786
30. Chen, M. F., and Chen, T. Y. (2001) Different fast-gate regulation by external Cl<sup>-</sup> and H<sup>+</sup> of the muscle-type ClC chloride channels. *J Gen Physiol* **118**, 23-32
31. Kang, I. S., Cho, J. H., Choi, I. S., Kim, D. Y., and Jang, I. S. (2016) Acidic pH modulation of Na<sup>+</sup> channels in trigeminal mesencephalic nucleus neurons. *Neuroreport* **27**, 1274-1280

- 1  
2  
3 32. Chauvigne, F., Zapater, C., Stavang, J. A., Taranger, G. L., Cerda, J., and Finn, R. N. (2015) The pH  
4 sensitivity of Aqp0 channels in tetraploid and diploid teleosts. *FASEB J* **29**, 2172-2184
- 5 33. Holzer, P. (2009) Acid-sensitive ion channels and receptors. *Handb Exp Pharmacol*, 283-332
- 6 34. Franz, M. C., Anderle, P., Burzle, M., Suzuki, Y., Freeman, M. R., Hediger, M. A., and Kovacs, G.  
7 (2013) Zinc transporters in prostate cancer. *Mol Aspects Med* **34**, 735-741
- 8 35. Charalabopoulos, K., Karachalios, G., Baltogiannis, D., Charalabopoulos, A., Giannakopoulos, X.,  
9 and Sofikitis, N. (2003) Penetration of antimicrobial agents into the prostate. *Chemotherapy* **49**,  
10 269-279
- 11 36. Boer, M., Duchnik, E., Maleszka, R., and Marchlewicz, M. (2016) Structural and biophysical  
12 characteristics of human skin in maintaining proper epidermal barrier function. *Postepy*  
13 *Dermatol Alergol* **33**, 1-5
- 14 37. Dufner-Beattie, J., Langmade, S. J., Wang, F., Eide, D., and Andrews, G. K. (2003) Structure,  
15 function, and regulation of a subfamily of mouse zinc transporter genes. *J Biol Chem* **278**, 50142-  
16 50150
- 17 38. Lane, D. J., Robinson, S. R., Czerwinska, H., and Lawen, A. (2010) A role for Na<sup>+</sup>/H<sup>+</sup> exchangers  
18 and intracellular pH in regulating vitamin C-driven electron transport across the plasma  
19 membrane. *Biochem J* **428**, 191-200
- 20 39. Vigliarolo, T., Zocchi, E., Fresia, C., Booz, V., and Guida, L. (2016) Abscisic acid influx into human  
21 nucleated cells occurs through the anion exchanger AE2. *Int J Biochem Cell Biol* **75**, 99-103
- 22 40. Lang, K., Wagner, C., Haddad, G., Burnekova, O., and Geibel, J. (2003) Intracellular pH activates  
23 membrane-bound Na<sup>(+)</sup>/H<sup>(+)</sup> exchanger and vacuolar H<sup>(+)</sup>-ATPase in human embryonic kidney  
24 (HEK) cells. *Cell Physiol Biochem* **13**, 257-262
- 25 41. Yabuuchi, H., Tamai, I., Sai, Y., and Tsuji, A. (1998) Possible role of anion exchanger AE2 as the  
26 intestinal monocarboxylic acid/anion antiporter. *Pharm Res* **15**, 411-416
- 27 42. Sobczak, K., Bangel-Ruland, N., Leier, G., and Weber, W. M. (2010) Endogenous transport  
28 systems in the *Xenopus laevis* oocyte plasma membrane. *Methods* **51**, 183-189
- 29 43. Giacconi, R., Muti, E., Malavolta, M., Cardelli, M., Pierpaoli, S., Cipriano, C., Costarelli, L., Tesei,  
30 S., Saba, V., and Mocchegiani, E. (2008) A novel Zip2 Gln/Arg/Leu codon 2 polymorphism is  
31 associated with carotid artery disease in aging. *Rejuvenation Res* **11**, 297-300
- 32 44. Karagas, M. R., Andrew, A. S., Nelson, H. H., Li, Z., Punshon, T., Schned, A., Marsit, C. J., Morris, J.  
33 S., Moore, J. H., Tyler, A. L., Gilbert-Diamond, D., Guerinot, M. L., and Kelsey, K. T. (2012)  
34 SLC39A2 and FSIP1 polymorphisms as potential modifiers of arsenic-related bladder cancer.  
35 *Hum Genet* **131**, 453-461
- 36 45. Kamei, S., Fujikawa, H., Nohara, H., Ueno-Shuto, K., Maruta, K., Nakashima, R., Kawakami, T.,  
37 Matsumoto, C., Sakaguchi, Y., Ono, T., Suico, M. A., Boucher, R. C., Gruenert, D. C., Takeo, T.,  
38 Nakagata, N., Li, J. D., Kai, H., and Shuto, T. (2018) Zinc Deficiency via a Splice Switch in Zinc  
39 Importer ZIP2/SLC39A2 Causes Cystic Fibrosis-Associated MUC5AC Hypersecretion in Airway  
40 Epithelial Cells. *EBioMedicine* **27**, 304-316
- 41 46. Hamon, R., Homan, C. C., Tran, H. B., Mukaro, V. R., Lester, S. E., Roscioli, E., Bosco, M. D.,  
42 Murgia, C. M., Ackland, M. L., Jersmann, H. P., Lang, C., Zalewski, P. D., and Hodge, S. J. (2014)  
43 Zinc and zinc transporters in macrophages and their roles in efferocytosis in COPD. *PLoS One* **9**,  
44 e110056
- 45 47. Girijashanker, K., He, L., Soleimani, M., Reed, J. M., Li, H., Liu, Z., Wang, B., Dalton, T. P., and  
46 Nebert, D. W. (2008) Slc39a14 gene encodes ZIP14, a metal/bicarbonate symporter: similarities  
47 to the ZIP8 transporter. *Mol Pharmacol* **73**, 1413-1423
- 48 48. He, L., Girijashanker, K., Dalton, T. P., Reed, J., Li, H., Soleimani, M., and Nebert, D. W. (2006)  
49 ZIP8, member of the solute-carrier-39 (SLC39) metal-transporter family: characterization of  
50 transporter properties. *Mol Pharmacol* **70**, 171-180
- 51  
52  
53  
54  
55  
56  
57  
58  
59  
60



For Table of contents use only

